Constructing Penrose-like tilings from a single prototile and the implications for quasicrystals

Hyeong-Chai Jeong
Institute for Physical Science and Technology, University of Maryland, College Park, Maryland 20742

Paul J. Steinhardt
Department of Physics and Astronomy, University of Pennsylvania, Philadelphia, Pennsylvania 19104
(Received 3 September 1996)

We present two sets of rules for constructing quasiperiodic tilings that suggest a simpler structural model of quasicrystals and a more plausible explanation of why quasicrystals form. First, we show that quasiperiodic tilings can be constructed from a single prototile with matching rules which constrain the way that neighbors can overlap. Second, we show that maximizing the density of a certain cluster of fat and thin tiles can force a Penrose tiling without imposing the usual Penrose matching rules. [S0163-1829(97)02706-9]

I. INTRODUCTION

Quasicrystals are solids with quasiperiodic translational order and crystallographically disallowed rotational symmetry. A leading model for describing their structure and properties has been the Penrose tiling picture,[1] based on the two-dimensional aperiodic pattern invented by Roger Penrose[2] in 1974. The Penrose pattern is composed of fat and thin rhombi with matching rules which constrain the way neighboring tiles can join together edge-to-edge. Penrose showed that the only plane-filling tiling consistent with those matching rules is uniquely the Penrose pattern. The generalization to three-dimensional structures with icosahedral symmetry composed of rhombohedral bricks with matching rules has been found. In the Penrose tiling picture, one imagines that the tiles represent two distinct clusters of atoms and the matching rules represent atomic interactions.

The Penrose tiling picture successfully explains all of the known structural and physical properties of quasicrystals, including the microscopic arrangement of atoms as viewed with scanning tunneling electron microscopy.[3,4] Nevertheless, serious theoretical doubts about its validity have remained. The physical conditions required to emulate a Penrose tiling appear to be much more complex than what is needed to form periodic crystals. For example, the Penrose tiling picture suggests that the atoms must organize into *two* distinct clusters which act as the building blocks of the quasicrystalline structure, whereas crystals require only a single building block. The condition for crystals seems intuitively simple: it is easy to imagine a single building block arising as a low-energy atomic cluster of the given elements. For quasicrystals, the energetics must be delicately balanced to allow two distinct clusters to intermix with a specific ratio of densities. Furthermore, the atomic interactions must restrict clusters so that they join only according to the matching rules. Concerns about these conditions have led to a proliferation of alternative models for quasicrystals, including the icosahedral glass, random tiling, and entropic pictures.[5] The alternatives all predict imperfect quasiperiodic structures with differing degrees and types of imperfection and they also predict that quasicrystals are metastable. Yet, recent, highly perfect quasicrystals have been discovered—as perfect as periodic crystals made of similar elements—and some appear to be thermodynamically stable. The peculiar situation has developed that the Penrose tiling picture has been increasingly supported observationally, while it has remained questionable theoretically.

In this paper, we discuss two schemes for constructing quasiperiodic tilings which address the theoretical criticisms of the Penrose tiling picture. Although the work presented here is, for the most part, an abstract study of the property of tilings, the results may profoundly influence our intuition about quasicrystals. First, in Sec. II, we present a simple proof of the claim[6] that a quasiperiodic tiling can be forced using only a single type of tile (plus matching rule). Second, in Sec. III, we show that matching rules can be discarded altogether. Instead, maximizing the density of a chosen cluster of tiles suffices. The results are surprising from a mathematical standpoint and suggest an explanation of why quasicrystals form. The basic conclusions were discussed in a short paper,[7] and here we produce the detailed proofs which establish the results.

In particular, the second approach suggests a simple thermodynamic mechanism for quasicrystal formation. If one imagines that the chosen cluster of tiles represents some energetically preferred atomic cluster, then minimizing the free energy would naturally maximize the cluster density and, thereby, force quasicrystallinity. We first show that the ground state is the perfect (Penrose-like) quasicrystal state if the clusters are assigned the same energy independent of local environment, as discussed in our short paper. In this case, maximizing density and minimizing energy are equivalent. In this paper, we also show the same ground-state results if different energies are assigned to the cluster depending on its local environment. This is a significant extension of our earlier results since some difference in cluster energies for different environments seems a natural idea. Conversely, it shows that the same maximum-density configuration is the ground state for a range of energetic assignments. This cluster model of quasicrystals had been conjectured previously by the authors,[8] and now it is proven to be mathematically possible. In our concluding remarks in Sec. IV, we discuss the implications of our mathematical result for future theoretical and experimental research in quasicrystals.

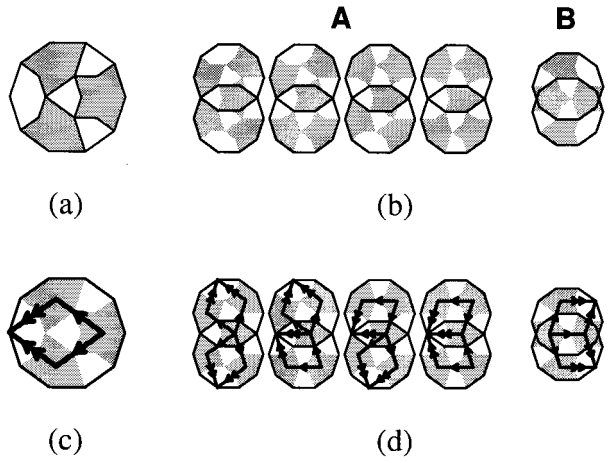

FIG. 1. A quasiperiodic tiling can be forced using marked decagons shown in (a) with overlapping rules. Overlapping rules demand that two decagons may overlap only if shaded regions overlap and if the overlap area is greater than or equal to the overlap region in *A*. This permits five types of pairwise overlaps, four types of *A* overlaps and one type of *B*-type overlap as shown in (b). If each decagon is inscribed with a fat rhombus, as shown in (c), the inscribed rhombi from two overlapping decagons share at least one vertex (d) and as much as a complete edge.

II. CONSTRUCTION SCHEME I: SINGLE TILE WITH A OVERLAPPING RULE

We first show that a quasiperiodic tiling can be forced using a single type of tile combined with an overlapping rule. Because neighboring tiles overlap, the result is an unconventional tiling, perhaps better termed a ''covering.''

As an analogy to a real atomic structure for quasicrystals, the overlaps should be construed as the sharing of atoms between neighboring clusters, rather than interpenetration of two complete clusters. This paper suggests that the sharing of atoms by clusters may be an important structural motif that may play an important role in the formation and stability of quasicrystals.

The construction was originally proposed by Gummelt, who presented an elaborate proof.[6] Our contribution is a very simple, alternative proof which makes clear the relation to Penrose tilings and leads us to a second scheme.

For our example, the single tile is chosen to be the decagon shown in Fig. 1(a). Unlike Penrose tiles, the decagons are permitted to overlap, but only in certain discrete ways. Two decagons may overlap only if similarly shaded regions overlap and the overlap area is greater than or equal to the hexagonal overlap area shown in *A*. Counting the relative orientations of the neighboring decagons, one finds that the overlap rule permits five types of nearest-neighbor configurations: four *A*-type overlaps and one *B*-type overlap as shown in Fig. 1(b). The *A* and *B* overlaps produce two different separations between the centers of neighboring decagons. Roughly speaking, these two distances, which have a relatively irrational ratio, replace the two tile types in the usual Penrose tilings.

Our proof that the overlap rules force uniquely a quasiperiodic tiling analogous to a Penrose tiling is based on inscribing each decagon with a Penrose fat rhombus tile marked with single and double arrows, as illustrated in Fig. 1(c). We remind the reader that the original Penrose tiling is constructed from fat and thin rhombi. Two edges may join together only if the type and direction of arrows match.[9,10] For any two overlapping decagons, the ''inscribed'' rhombi share at least one vertex and sometimes share an edge. Where the rhombi join at a vertex only, there is an open angle formed by the edges which are the location and shape where rhombi can be fit according to the Penrose matching rules as shown in Fig. 1(d). For these ''implied'' rhombi, the arrows are fixed by the arrows on adjoining inscribed rhombi.

We will show that the overlap rules force precisely the same nearest-neighbor configurations of inscribed and implied rhombi as do the Penrose edge-matching rules. Gummelt showed that there are exactly 20 different ways a given decagon can be surrounded by neighbors, where surrounding a decagon means the edges of the decagon is covered by the interior of other decagons by *A* or *B* overlaps.[6] Figures 2(a)–2(c) show all 20 ways of surrounding a decagon with corresponding rhombus tile configurations. These 20 allowed decagon configurations have been broken into three groups.

The first nine decagon configurations [Fig. 2(a)] are in one-to-one correspondence with the nine ways of surrounding the fat rhombus inscribed in the central decagon by neighboring fat and thin rhombi according to the Penrose matching rules. By ''surrounding'' a rhombus, we mean that all four of its edges are joined to neighboring rhombi with matching arrows; furthermore, three of its vertices must be surrounded by corners of neighboring rhombi. The neighboring rhombi may be inscribed in neighboring decagons or implied. The fourth vertex (at which the two double-arrow edges of the central rhombus meet) is not completely surrounded in some of the nine configurations. Later, we discuss how this last vertex is also forced to be a Penrose-like configuration when one applies the overlap rules beyond the central decagon to neighboring decagons.

The next eight decagon configurations are shown in Fig. 2(b). The inscribed rhombi of the central decagon in this group are only partially surrounded. However, when the decagon overlap rules are applied to neighbors of the central decagon, the result is one of the nine ways of completely surrounding the central rhombus, as discussed in the first grouping. Hence, these eight configurations do not add any new constraints beyond what is already imposed by the first nine configurations.

The remaining three configurations are shown in Fig. 2(c). These configurations of inscribed and implied rhombi display no matching rule violation. However, they never occur in a perfect Penrose tiling. This is because a mismatch is inevitable if one continues to add rhombi. Similarly, the three configurations of decagons do not occur in a perfect decagon tiling because, if one continues to add decagons, a decagon overlap-rule violation is inevitably forced; that is, some neighboring decagons cannot be surrounded by one of the 20 configurations. Hence, the three configurations play equivalent roles in decagon tilings and Penrose rhombus tilings.

We have shown that all decagons in a perfect decagon tiling are surrounded by one of the first nine configurations in Gummelt's list. In three of these configurations (Configu-

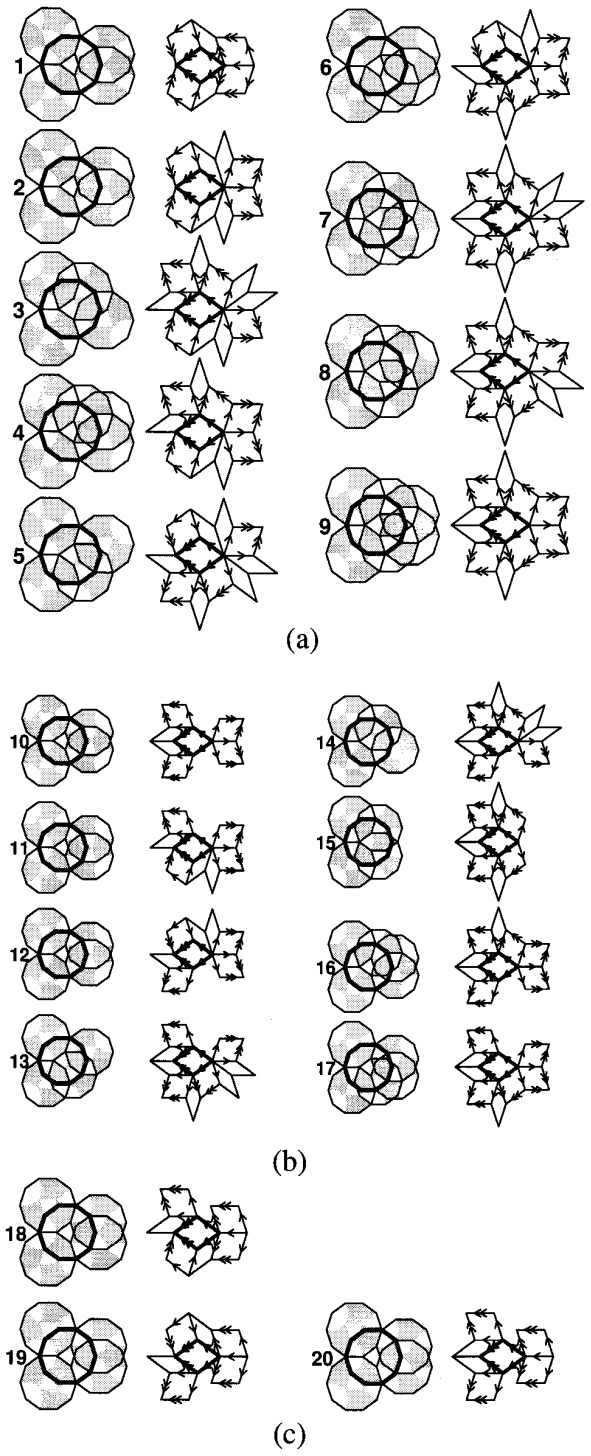

FIG. 2. Twenty ways of surrounding a decagon and corresponding rhombus tile configurations. (a) First group; central fat rhombi are surrounded by fat and thin rhombi according to the Penrose matching rules. (b) Second group; center decagons are surrounded by other decagons but the central rhombi are only partially surrounded. Each configuration is a subconfiguration of one of the nine configurations in (a), and so imposes no new constraints. (c) Third group; any way of adding decagons to these three configurations forces a mismatch. Similarly, any way of adding rhombi to the rhombus configuration forces a mismatch (e.g., some open angles formed by the edges of fat rhombi cannot be filled by arrow matched rhombi). Hence, these configurations never appear in a perfect tiling.

ration 7, 8, and 9), the central inscribed rhombus is surrounded on all edges and all four vertices by neighboring rhombi. So these map into a unique, Penrose rhombus configuration. In the remaining six configurations, the fourth vertex is incomplete. For four of the six cases (Configuration 3, 4, 5, and 6), simple experimentation shows that there is a unique way to complete the fourth by applying the same overlap rules to one of the neighboring decagons. For the remaining two configurations, Configuration 1 and 2, there are two distinct allowed ways of adding overlapping decagons so that the inscribed rhombi complete the vertex. The two configurations of inscribed decagons are also distinct, but each corresponds to an allowed Penrose configuration. Counting all of these, the nine decagon configurations map into 11 ways of completely surrounding a central fat rhombus by neighboring rhombi, precisely the number and types allowed by the Penrose arrow rules. [One of the 11 rhombus configurations, does not occur in a perfect Penrose tiling nor does the analogous decagon configuration occur in a perfect decagonal tiling. Although the configuration itself obeys the matching rules (overlap rules), it is impossible to add the configuration without ultimately producing a matching rule (overlap rule) violation.] That is, restricting the surroundings of every fat rhombus to these 11 types is equivalent to enforcing the Penrose arrow rules for fat rhombi; in a Penrose tiling, every thin tile adjoins fat tiles, so fixing the surrounding of every fat rhombus automatically fixes the environment of every thin rhombus. Hence, the decagon overlap rules are equivalent to Penrose arrow rules, and the proof is completed.

A significant corollary is that the two-tile Penrose tiling can be reinterpreted in terms of a single, repeating motif. The analog for quasicrystals is that the atomic structure, which has been described in terms of two or more cluster units in the past, can be reinterpreted in terms of a single, repeating atomic cluster. This reinterpretation of the structure itself is a simplification which is valid independent of whether overlap energetics is an important factor in quasicrystal formation or not.

III. CONSTRUCTION SCHEME II: MAXIMIZING CLUSTER DENSITY

Here we show the Penrose matching rules can be replaced by a different tiling principle and still obtain the same tiling. Namely, if one allows any possible configuration of fat and thin rhombi, a perfect Penrose tiling can be picked out by maximizing the density of a particular tile cluster. As a model for quasicrystals, the notion is that the chosen cluster represents some low-energy, microscopic cluster of atoms. Minimizing the energy naturally maximizes the cluster density and forces quasiperiodicity. Our result suggests that the energetic conditions required for quasicrystal formation are only that a single chosen cluster be low energy, which is similar to the conditions needed to form periodic crystals and simpler to envisage than the conditions needed to form two different tiles plus matching rules.

For this paper, we will focus on the tile cluster, C, defined as

Definition. A C cluster is composed of five fat and two thin rhombi plus two side hexagons composed of two fat and

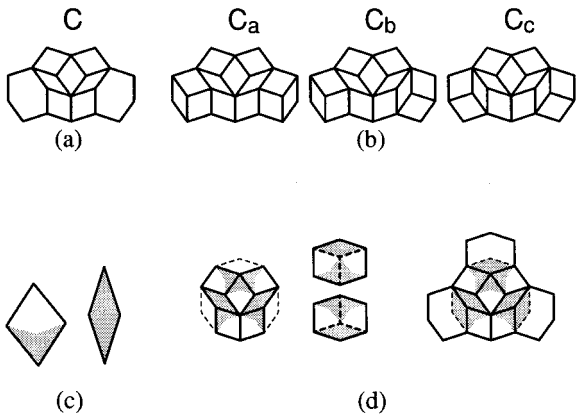

FIG. 3. (a) A C cluster consists of five fat and two thin rhombi with two side hexagons composed of two fat and one thin rhombus each. There are two possible configurations for filling each side hexagon. This gives rise to three types, C_a, C_b, and C_c, depending on the orientation of the tiles within the two side hexagons (b). Shade a dart-shaped region in each fat rhombus and the entire interior of each thin rhombus as shown in (c). For a particular choice of orientations for the fat rhombi, the resulting shadings within a C cluster join together in a pattern that is equivalent to that of an overlaid, marked decagon that circumscribes the central seven tiles, as shown in (d).

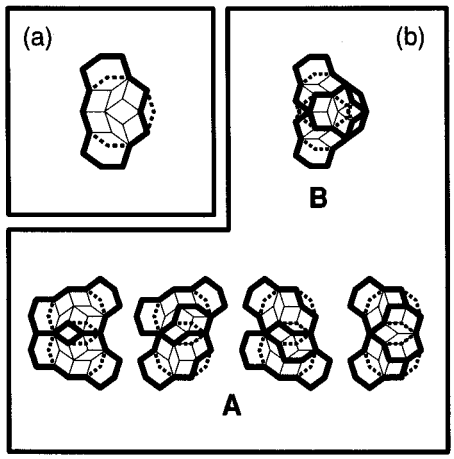

FIG. 4. (a) Shows a C cluster with a decagon circumscribing the central seven rhombi. The center of the C cluster is defined to be the center of the decagon. (b) Shows the two kinds of overlaps between C clusters which bring the centers closest together. (The A types have the same separation between centers.) If decagons are circumscribed about the central seven rhombi of each C cluster, the A- and B-type overlaps between C clusters transform into precisely the A- and B-type overlaps between decagons described in the previous section.

one thin rhombus each, as shown in Fig. 3. Penrose tiling experts will recognize the central seven tiles as being a Jack configuration and the central decagon as being a ''cartwheel.'' [11] It should be emphasized that this is only a particular example of a tile cluster that suffices; other choices are possible.

Our central proposition is

Proposition. The Penrose tiling uniquely has the maximum density of C clusters among tilings constructed from Penrose rhombi. The density is defined as the number of C clusters per unit area. Two tilings are considered to be distinct only if they differ from one another by patches whose density has nonzero measure.

Our choice for the C clusters was motivated by the overlapping decagons described in the previous section. The C clusters in a Penrose tiling and the decagons in a decagon tiling (Scheme I) are in one-to-one correspondence. That is, if decagons are placed so that they circumscribe the central seven tiles of the C cluster, the decagons form a perfect decagon tiling obeying the overlap rules described in the previous section. Although the decagon and C cluster have different exterior shapes, their key similarity is that two neighboring C clusters can share tiles in two ways isomorphic to the A and B overlaps of decagons; see Fig. 4.

Figures 3(c) and 3(d) show the relation between a marked decagon and a C cluster. Consider the central seven tiles of the C cluster. Shade a dart-shaped region in each fat rhombus and the entire interior of each thin rhombus as shown in Fig. 3(c). For a particular choice of orientations for the fat rhombi, the resulting shadings within a C cluster join together in a pattern that is equivalent to that of an overlaid, marked decagon that circumscribes the central seven tiles, as shown in Fig. 3(d). (We have added a third hexagon anticipating our result that two side hexagons guarantee the third hexagon in a tiling with maximum density of C clusters; see Sec. III C)

In broad outline, our formal proof of the proposition is based on the properties of tilings under ''deflation.'' Deflation corresponds to replacing each complete C cluster by a larger, ''deflated'' fat rhombus using a slight generalization of the self-similar substitution rules introduced by Penrose. The deflated rhombi form a new tiling (with holes, in general) which can be deflated again. We show that, if there were a tiling with a greater density of C clusters than Penrose tiling, then deflating the tiling increases the density further. Repeated deflation leads to an unbounded density, which is impossible. Hence, there can be no tiling with greater density of C clusters than Penrose tiling. Then we show that the Penrose tiling is the unique one which has the maximum density of C clusters.

A. Terminology and notation

For the details of the proof, it is useful to introduce some specialized terminology and notation.

(i) $C_{(a,b,c)}$: By definition, a tile cluster is identified as a C cluster independent of the orientation of its side hexagons. However, for the purpose of proof, it is useful to distinguish three types of C clusters depending on which way the side hexagons are flipped: C_a, C_b, and C_c as shown in Fig. 3(b). The reflection of C_b around the vertical axis is also considered to be type C_b.

(ii) ρ and R: For any given configuration X, we use ρ_X to represent the number per unit area where an acute rhombus has area equal to unity; and we use R_X be the number per C cluster. For example, ρ_C is the number of C clusters per unit area. Note that $R_C=1$ by definition. To refer to the values of ρ and R in a perfect Penrose tiling, we add a superscript: ρ^0 and R^0. For example,

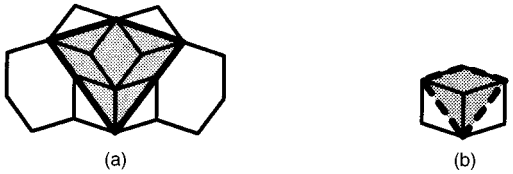

FIG. 5. (a) C-kite; (b) H-kite.

$$\rho_C^0 = 1/(3\tau+1),$$

$$\rho_B^0 = 1/[\tau^2(3\tau+1)],$$

$$R_B^0 = 1/\tau^2,$$

where $\tau=(1+\sqrt{5})/2$ is the golden ratio and subscript B refers to pairs of neighboring C clusters with B overlaps. (B overlaps play an important role in the proof.)

(iii) Area per configuration, $A(\alpha)$: $A(\alpha)$ represents the area of a configuration α. $\alpha\cup\beta$ is the union of configurations α and β. For example,

$$A(C) = 9\tau+4,$$

(iv) C-kites (K_C) and H-kites (K_H): Because the C clusters can overlap, it is important for the proof to have a reliable scheme for assigning, or at least bounding the area occupied by a given C cluster. A useful trick is to decorate each C cluster with the kite-shape shadings shown in Fig. 5. A C-kite, K_C, is the shaded subregion of a C cluster shown in Fig. 5(a). For any two C clusters which do not have a B overlap, the associated C-kites do not overlap. Hence, if a given C cluster has no B overlaps whatsoever, it can be assigned at least the area of K_C. Conversely, the only way a C cluster can be assigned less area than K_C is if it has B overlaps.

An H-kite, K_H, refers to the shaded subregion of a hexagon belonging to a C cluster as shown in Fig. 5(b). We apply the term H-kite only to hexagons which belong to some C cluster. Note that

$$A(K_C) = \tau^4,$$

$$A(K_H) = \tau^2.$$

(v) Deflation: ''Deflation,'' as used in this paper, is a transformation in which each C cluster is replaced by a large fat rhombus, as shown in Fig. 6(a). The large rhombus will be referred to as the ''deflated rhombus.'' Note that the deflated rhombus replacing one C cluster is unable to overlap the deflated rhombus replacing any other C cluster no matter how the two are juxtaposed or overlapped.

This definition of deflation is closely related to the self-similar inflation and deflation operations introduced by Penrose. The Penrose operations produce both deflated fat and thin rhombi, whereas here we only introduce the fat rhombi. The Penrose deflation operation acting on a perfect Penrose tiling produces a scaled-up version of a perfect Penrose tiling composed of deflated fat and thin rhombi, demonstrating its self-similar structure. Penrose's operation is defined only for Penrose tilings and subconfigurations. Our deflation operation acting on a perfect Penrose tiling reproduces the scaled-up fat rhombi, but does not explicitly construct scaled-up thin rhombi. Instead, holes are left between the deflated fat rhombi where the thin rhombi fit. It is a minor difference if one is only considering perfect Penrose tilings. For more general tilings, as must be considered in this proof, the difference is more significant. Our deflation is defined for Penrose and non-Penrose. In either case, one obtains an arrangement of deflated rhombi separated by spaces or holes; but, the holes do not have to be shaped so that scaled-up thin rhombi fit, in general.

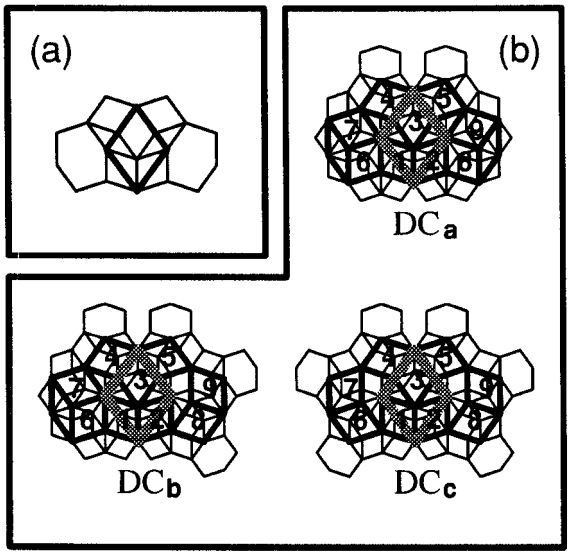

FIG. 6. Deflation replaces each C cluster with a large, fat rhombus, as shown in (a). A deflated C cluster DC is composed of the nine deflated rhombi obtained by replacing each of nine C clusters numbered from 1 to 9 with a fat rhombus, as shown in (b). The DC cluster can be deflated again by replacing it with the very large rhombus (doubly deflated tile) shown in (b).

(vi) Deflated C cluster, DC: The deflation operation can be repeated. Identify all configurations of deflated rhombi which form a scaled-up version of the C cluster, as shown in Fig. 6, and replace with a yet larger, fat rhombus: a doubly deflated rhombus. We call the group of nine C clusters a ''deflated C cluster,'' DC. The positions of the first five C clusters in the DC relative to one another is fixed, but the pairs on either side can be flipped independently, just as side hexagons can be independently flipped in a C cluster. This results in three kinds of DC clusters, DC_a, DC_b, and DC_c. Repeated deflations are defined analogously.

B. Proving the maximum density proposition

The first goal is to prove that $\rho_C \leq \rho_C^0$ for any definite tiling. Then, we show that the Penrose tiling is the unique tiling with $\rho_C = \rho_C^0$.

1. An overview

To obtain a lower bound on the average area occupied per C clusters, we sum the C-kite subareas and divide by the number of C's, correcting for cases where C-kites overlap. The C-kite is a subregion of a C cluster with area $3\tau+2$; we can consider it to be a core area of the C cluster which is only overlapped by a neighboring C-kite if there is a B

overlap. More precisely, although C clusters can overlap to some degree, the only possibilities for close overlap are A overlaps, in which the corresponding C-kites meet along an edge; or B overlaps, in which a specific overlap of C-kites occurs (recall Fig. 4). In a Penrose tiling, the C-kites fill the entire plane without holes. If the C-kite is not overlapped by any neighboring one, the corresponding C cluster can be assigned the entire area of a C-kite (at least that); for these cases, the C clusters occupy area $\geqslant 3\tau+2$, so they decrease the density relative to the Penrose value $\rho_C=1/(3\tau+1)$. Two C clusters with B overlaps are assigned area less than $3\tau+1$ due to the overlap of their C-kites. Hence, we reach an important conclusion: B overlaps are the only mechanism for exceeding Penrose density.

To exceed the Penrose density, a tiling must have more B overlaps than in a Penrose tiling. However, this condition is not sufficient. In Penrose tiling, every B overlap of two C clusters is surrounded by a DC cluster. In a non-Penrose tiling, a fraction of B overlaps may not be part of a DC cluster (i.e., one or more of the seven other C clusters that compose a DC cluster is absent). In these cases, it is necessary to show by explicit constructions that one can always identify ''extra'' area ''P'' nearby the associated B overlap which does not belong to the C-kite of any C cluster and is not associated with any other B overlap. This important part of the argument is detailed in the next subsection. The ''extra,'' unassigned area occupies at least as much area as saved by the B overlap. Hence, a B overlap which is not part of a DC cluster does not contribute to decreasing the density of C clusters below the Penrose value.

Suppose there were a tiling with a density of C clusters greater than the Penrose value. Then, it must have a higher density of DC clusters than in a Penrose tiling, $R_{DC}>\tau^{-2}$, where R_{DC} is the number of DC clusters divided by the number of C clusters. Under deflation and rescaling the area by τ^2, each DC cluster becomes a C cluster of the deflated tiling whose density is $\tau^2 R_{DC}\rho_C$. Since $R_{DC}>\tau^{-2}$, the deflated tiling has a density of C clusters that is strictly greater than the original tiling. Repeating the deflation *ad infinitum* would lead to a tiling with an unbounded density of C clusters. This is impossible (since C clusters occupy finite area), and so there can be no tiling with higher C-cluster density. A corollary is that, if the C-cluster density equals the Penrose value, then $R_{DC}=\tau^{-2}$ (the Penrose tiling value) and the C-cluster density in the *deflated* tiling must also equal the Penrose value. This corollary is then used to establish that the Penrose tiling is the unique configuration with the maximal density value.

2. Formal argument

Let χ_m be a hypothetical tiling which has the $\rho_C>\rho_C^0$. We set out to prove:

Theorem 1. In χ_m, $R_{DC}>\tau^{-2}$. If Theorem 1 holds, then the density of DC clusters in tiling χ_m is $\rho_{DC}=R_{DC}\rho_C>\tau^{-2}\rho_C$. Under deflation, each DC cluster becomes a C cluster composed of deflated tiles. If we rescale the deflated rhombi by τ^2 so that they have the same area as the original rhombi, the resulting tiling has a density of C clusters $\tau^2\rho_{DC}$ which is strictly greater than ρ_C. Repeated deflation leads to a sequence of tilings with increasing C cluster density without bound, which is impossible. Hence,

FIG. 7. An H-kite (dark grey) is either a subarea of a C-kite (light grey)—the two ways shown in 6(a) and 6(b) above—or it has no overlap with a C-kite at all.

Theorem 1 is the key to proving that χ_m is impossible and all tilings must have $\rho_C\leqslant\rho_C^0$. We build to Theorem 1 through a series of subsidiary theorems.

By checking all hexagons which may share a tile with C clusters, it is straightforward to see that:

Lemma 1: For a given H-kite, there are only two ways that it can overlap with a C-kite, shown in Fig. 7.

Corollary 1.1 An H-kite is completely overlapped by a C-kite or it has no overlaps with C-kites at all.

Definition. Configuration n is the union of C clusters from 1 to n as enumerated in Fig. 6(b) ($n=1,\ldots,9$). The number order in the figure is significant. R_n is the R value of Configuration n. By definition $R_1=1$. R_2 means R_B, the pairs of C clusters (belonging to a DC cluster) with B overlap.

Theorem 2. In χ_m, $R_2>\tau^{-2}$.

Proof: The overlap between the C-kites of any two C clusters with a B overlap corresponds to an H-kite with area τ^2. All other C-kites do not overlap. Hence, the fractional area occupied by C-kites overall, $a1\equiv A(\cup K_C)/A(\chi_m)$, is given by

$$a1=\rho_C(\tau^4-R_2\tau^2).$$

(That is, area τ^4 for each C-kite minus area τ^2 for each B overlap.) Since $a1\leqslant 1$ by definition and $\rho_C>\rho_C^0$ by assumption, $R_2\tau^2$ must be greater than 1 [note that $\rho_C^0=1/(3\tau+1)=1/(\tau^4-1)$]. Hence, $R_2>\tau^{-2}$.

This proves that the number of B overlaps per C cluster, R_2, must exceed τ^{-2} in order for tiling χ_m to have $\rho_C>\rho_C^0$. This is necessary because only B overlaps bring C clusters close enough together to exceed the Penrose density of C clusters locally. But, $R_2>\tau^{-2}$ is not sufficient to prove that $\rho_C>\rho_C^0$: the area saved by a given B overlap may be compensated by other areas which do not belong to any C cluster.

In fact, we claim that exactly this happens if a B overlap is not surrounded by the seven other C clusters needed to form a DC cluster about it. We first consider the case of B overlaps in Configuration 2 (B overlapped) clusters for which C cluster number 3 in Fig. 6 is missing. We show that each such B overlap is compensated by ''extra area'' P_2 adjoining the Configuration-2 cluster which is not assigned to any other C cluster. We then repeat a similar argument for cases of Configuration-3 clusters where C clusters 1 through 3 are present, but 4 is missing, etc. We identify ''extra area'' P_3, P_4, etc., and use this to show R_3, R_4, etc., all must exceed τ^{-2}. Each case in the sequence requires its own detailed analysis, although the basic structure of the argument is the same. We stop once we have shown that $R_{DC}\equiv R_g>\tau^{-2}$. Then, our deflation argument described in the previous subsection can be applied.

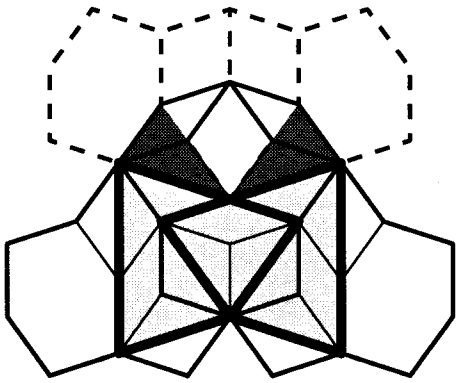

FIG. 8. The assignment of ''extra area'' P_2 as described in proof of Theorem 3.

The technically complicated part of the proof is checking that ''extra area'' is not double counted; that is, P_i must not overlap any other P_j with $j \leq i$. If it does, we must identify an alternative choice for P_i. This is done on a case by case basis below. In some cases, we may state that it is ''impossible'' for P_i and P_j to overlap. By impossible, we mean one of two conditions: (a) it is geometrically impossible to juxtapose a Configuration-i and Configuration-j cluster so that P_i and P_j overlap; or, (b) it is geometrically possible to join the Configuration-i and Configuration-j clusters, but then an additional C cluster is forced in between. P_i is defined only for Configuration i which are not part of a Configuration $i+1$; but joining a Configuration i onto a Configuration j transforms the Configuration-i cluster to a Configuration-$i+1$ cluster. Lemma 2 is an explicit example of (b). After Lemma 2, we simply state when an overlap is impossible without specifying whether the reason is (a) or (b).

Theorem 3. In χ_m, $R_3 > \tau^{-2}$.

Proof: Figure 8 shows a Configuration-2 cluster which is not included in a Configuration-3 cluster. The rhombi with solid lines belong to the Configuration 2. Dashed-line rhombi would also be there if this cluster were included in a Configuration 3. Since it is not, one or more of the dashed-line rhombi must be missing. Then the dark, shaded region is ''extra area'' P_2 which is not assigned to any C cluster. The extra area, with magnitude τ^2, compensates for the area saved by the B overlap between C_1 and C_2.

Then $A(P_2) = \tau^2$ and $R_{P_2} = R_2 - R_3$ since any two P_2's do not overlap. Let $a2$ be the fractional area occupied by the union of all K_C's and P_2's. From Theorem 2, we know $R_2 > \tau^{-2}$. Now we have

$$a2 = \rho_C[\tau^4 - R_2\tau^2 + (R_2 - R_3)\tau^2] = \rho_C(\tau^4 - R_3\tau^2),$$

Since $a2 \leq 1$, we have $R_3 > \tau^{-2}$.

Theorem 4. In χ_m, $R_4 > \tau^{-2}$.

Proof: Figure 9 shows a Configuration 3 which is not included in a Configuration 4 in part (a). The rhombi with solid lines belong to Configuration 3. Dashed-line rhombi would also be there if this were a subconfiguration of a Configuration 4. Since the Configuration 3 is not included in a Configuration 4, one or more of the dashed rhombi must be missing. Then, the dark, shaded region is ''extra area'' P_3 provided that this area does not overlap any other P_2 or P_3 assigned to another configuration. This must be checked. It is possible for the region shaded in (a) to overlap a P_2 from a neighboring Configuration 2, as illustrated in (b). But, then, it is possible to make a different, choice of P_3 which is not overlapped, as shown by the dark shading in (b). Another possibility is that the shaded region in (a) overlaps a P_3 belonging to a neighboring Configuration 3, as shown in (c). Once again, a different, choice of P_3 that is not overlapped can be made, as shown by the dark shading. In any case, there is always a region P_3 of area τ^2 which can be assigned to any Configuration 3 that does not belong to a Configuration 4.

The R value for P_3 is $R_3 - R_4$. From Theorem 3, we know $R_3 > \tau^{-2}$. Let $a3$ be the area density occupied by K_C's, P_2's, and P_3's. Then, we have

$$a3 = \rho_C[\tau^4 - R_3\tau^2 + (R_3 - R_4)\tau^2] = \rho_C(\tau^4 - R_4\tau^2).$$

Therefore, $R_4 > \tau^{-2}$.

Theorem 5. In χ_m, $R_5 > \tau^{-2}$.

Proof: Figure 10(a) shows a Configuration 4 which is not included in a Configuration 5. The rhombi with solid lines belong to Configuration 4. Dashed-line rhombi would also be there if this were a subconfiguration of a Configuration 5. Since it is not, one or more of the dashed rhombi must be missing. Then, the dark, shaded region is ''extra area'' P_4 provided that this area does not overlap any other P_2, P_3, or P_4 assigned to a neighboring configuration. Lemma 2 shows that it is impossible for a P_4 to overlap a P_3, leaving two cases. Figure 10(b) shows the case where the shaded region in (a) overlaps a P_2 belonging to a neighboring Configuration 2. In this case, a different, choice of P_4 can be made, as shown by the dark shading in (b). Similarly, Fig. 10(c) shows the case where the shaded region in (a) overlaps a P_4 belonging to a neighboring Configuration 4. Then a different, unoverlapped choice of P_4 can be made, as shown by the dark shading in (c). In any case, there is always a region P_4 of

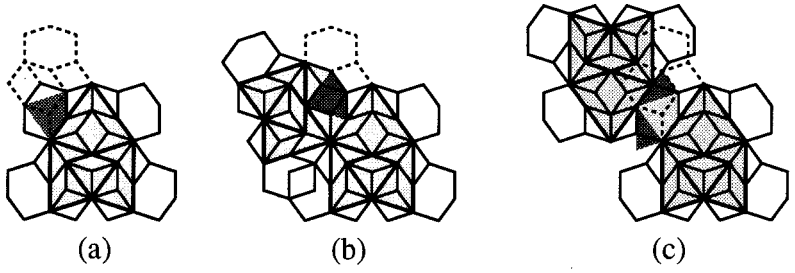

FIG. 9. The assignment of ''extra area'' P_3 as described in proof of Theorem 4.

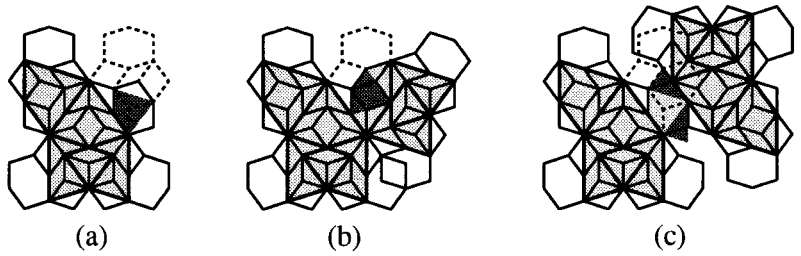

FIG. 10. The assignment of ''extra area'' P_4 as described in proof of Theorem 5.

area τ^2 which can be assigned to any configuration 4 that does not belong to a configuration 5.

Since any two P_4's do not overlap, $R_{P_4}=R_3-R_4$. From Theorem 4, we know $R_4>\tau^{-2}$. Let $a4$ be the area density occupied by K_C's, P_2's, P_3's, and P_4's. Then, we have

$$a4=\rho_C[\tau^4-R_4\tau^2+(R_4-R_5)\tau^2]=\rho_C(\tau^4-R_5\tau^{-2}).$$

Therefore, $R_5>\tau^{-2}$.

Lemma 2. A P_4 cannot overlap any P_3.

Proof: Figure 11 illustrates what happens if one were to try to bring together a Configuration 3 with a P_3 and a Configuration 4 with a P_4 so that P_3 and P_4 overlap (in the shaded region). Different cases must be analyzed because, for example, P_4 may be an H-kite, as in Fig. 10(a), or P_4 may have a different shape, as in Figs. 10(b) and 10(c). [Note: P_4 in Fig. 10(b) has the same geometrical shape as in Fig. 10(a), but it is not an H-kite because it does not belong to a hexagon which is part of a C cluster. Similarly, only in Fig. 9(a) does P_3 correspond to an H-kite.]

If P_4 and P_3 are both H-kites, an overlap is not possible because it forces a tile conflict at X. If one is an H-kite shape but not the other, a similar conflict results.

The remaining case to consider is if the P_4 of a Configuration 4 and the P_3 of a Configuration 3 do not correspond to an H-kite, as in Fig. 9(b) or Fig. 10(b). [Overlaps are not possible if P_3 corresponds to the case shown in Fig. 9(c) or P_4 corresponds to the case in Fig. 10(c).] This case occurs where there is also the overlap of a P_2 belonging to a third, Configuration-2 cluster. Here, it is geometrically possible to join the Configuration-3 and Configuration-4 clusters, but then an additional C cluster is forced in between, as shown in Fig. 11(b). The Configuration 4 is transformed into a Configuration 5, and so there is no P_4 region to identify. (Recall, P_4 is only defined for Configuration-4 clusters that are not part of a Configuration 5.) Thus, there is never a case where P_4 and P_3, as defined in the previous theorems, can overlap.

Theorem 6. In χ_m, $R_6>\tau^{-2}$.

Proof: Figures 12 and 13 illustrate a Configuration 5 which is not included in a Configuration 6, showing P_5 provided that this area does not overlap any other P_2, P_3, P_4, or P_5 assigned to another configuration. The markings in (a) for each figure are defined as in previous figures. Figure 12 covers the case where the C_1 cluster in the Configuration 5 is type C_a; Fig. 13 covers the case where it is type C_b.

Let us first consider Fig. 12: If the shaded region in (a) overlaps a P_2 belonging to a neighboring Configuration 2, as shown in (b), then a different, unoverlapped choice of P_5 can be made, as shown by the dark shading. If the shaded region in (a) overlaps a P_4, there are two possibilities depending on whether the P_4 corresponds to case (a) or (b) in Fig. 10; in either case, a different unoverlapped choice of P_5 can be made as shown in the dark shading in (c) or (d), respectively. If the P_4 corresponds to case (c) in Fig. 10, it cannot also overlap a P_5. If the shaded region in (a) overlaps another P_5 there is only the possibility shown in (e) and the choice of P_5 for one of the Configuration-5 clusters can be made differently, as shown by the dark shading.

Next, let us consider Fig. 13: The only geometric possibilities for overlap are if the shaded region in (a) overlaps a P_4 of a neighboring cluster of the type shown in Fig. 10(a) or a P_5 of a neighboring cluster, similar to Fig. 12(e). For each case, a different, unoverlapped choice of P_5 can be made, as shown by the dark shading in (b) and (c). In any case, a P_5 does not overlap with any P_i for $i<5$ and any two P_5's do not overlap each other. Since $R_{P_5}=R_5-R_6$, and, from Theorem 5, we know $R_5>\tau^{-2}$, we have

$$\rho_C[\tau^4-R_5\tau^2+(R_5-R_6)\tau^2]\leqslant 1,$$

and we have $R_6>\tau^{-2}$.

Theorem 7. In χ_m, $R_7>\tau^{-2}$.

Proof: Figure 14 shows a Configuration 6 which is not included in a Configuration 7 for the case where the C_1 cluster is type C_a in part (a) and for the case where the C_1 cluster is type C_b in part (b). In both cases, the ''extra area'' P_6 is shown for cases in which this area does not overlap any other

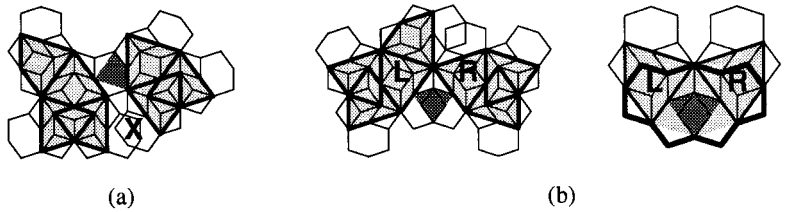

FIG. 11. Two cases considered in Lemma 2. Overlap between P_4 and P_3 is ruled out because there is a geometrical conflict between tiles [marked X in (a)], or because juxtaposing configurations force new C clusters where the P_4 and P_5 were supposed to overlap [shaded region in (b)]. See proof of Lemma 2 for discussion.

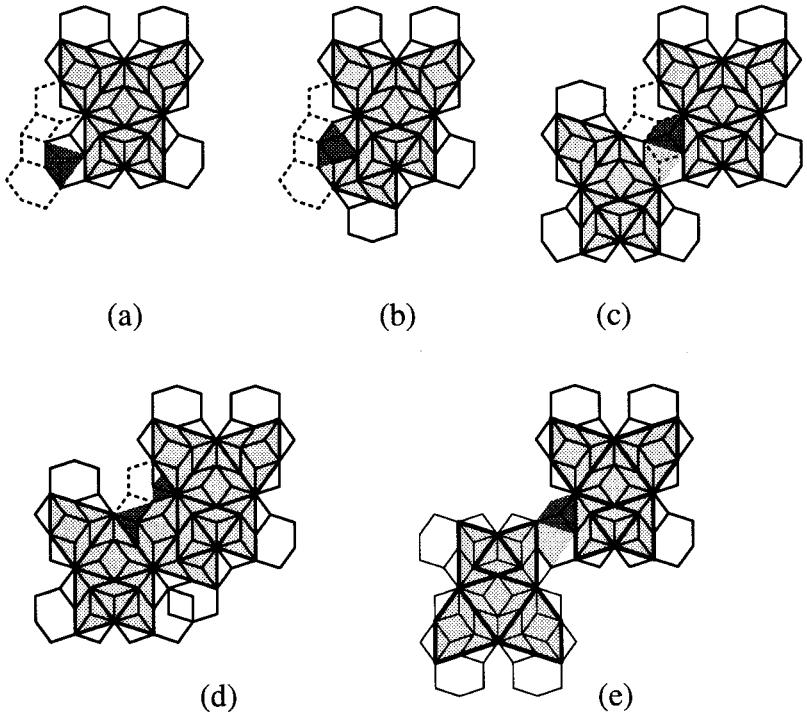

FIG. 12. The assignment of ''extra area'' P_5 if the C_1 cluster is type C_a, as described in proof of Theorem 6.

P_2 through P_6 assigned to another configuration. If the C_1 cluster is type C_a, there is no possible overlap with another P_i. If the C_1 cluster is type C_b, the only possible overlap is with the P_3 of a neighboring Configuration 3, in which case a different, choice of P_6 can be made, as shown by the dark shading in (c).

Since P_6 can always be defined such that it does not overlap other P_i, $i \leqslant 6$, the R value for P_6 is $R_{P_6} = R_6 - R_7$. From Theorem 6, we know $R_6 > \tau^{-2}$.

$$\rho_C[\tau^4 - R_6\tau^2 + (R_6 - R_7)\tau^2] \leqslant 1,$$

and we have $R_7 > \tau^{-2}$.

Theorem 8. In χ_m, $R_8 > \tau^{-2}$.

Proof: From Fig. 6, one sees that C_6 and C_8 are mirror images with respect to the vertical line bisecting the B overlap. Recall that P_5 (or P_7) is extra area defined when C_6 (or C_8) is missing. So the analysis of cases where P_7 overlaps P_i for $i = 2,3,4$ is similar to those for P_5. (To be precise, the case of overlap between P_7 and P_2 is equivalent to P_5 and P_2; between P_7 and P_3 is equivalent to P_5 and P_4; and between P_7 and P_4 is equivalent to P_5 and P_3.)

The new checks are for the case where P_7 (corresponding to an H-kite) overlaps with a P_5. In this case, as shown in Fig. 15(a), we can find the dark region which does not overlap with any P_i for $i \leqslant 6$. Also, it is possible for two P_7's to overlap; we have not illustrated the resolution of this case because it is similar geometrically to the case of two P_5's overlapping (see Theorem 6). By similar analysis to the previous theorems, we obtain $R_8 > \tau^{-2}$.

Finally, we are prepared to prove Theorem 1:

Theorem 1. In χ_m, $R_{DC} \equiv R_9 > \tau^{-2}$.

Proof: C_9 is in a position that is a mirror to C_7 in the deflated C cluster, so the analysis for P_8 is similar to P_6 in Theorem 7, so far as cases of overlap with any P_i for $i < 6$. The only case of overlap of P_8 with P_i for $i \geqslant 6$ is P_8 (corresponding to an H-kite) overlapping with P_6. In this case, as shown in Fig. 15(b), we can identify the shaded region which does not overlap with any P_i for $i \leqslant 7$. It is not geometrically possible to arrange two P_8's to overlap.

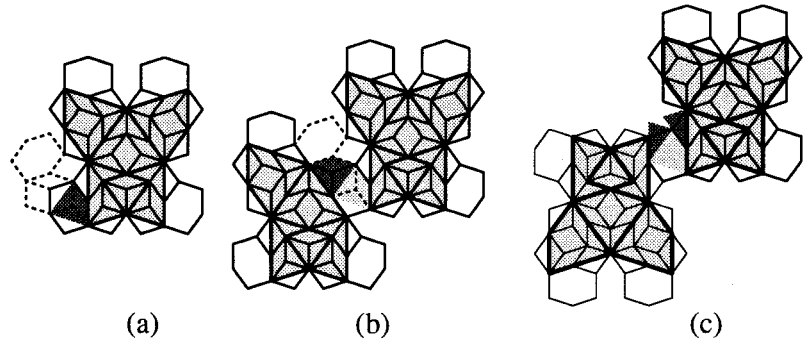

FIG. 13. The assignment of ''extra area'' P_5 if the C_1 cluster is type C_b, as described in proof of Theorem 6.

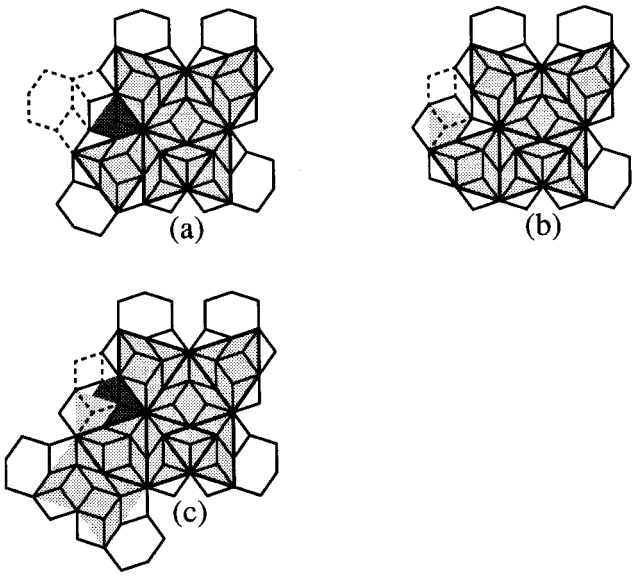

FIG. 14. The assignment of ''extra area'' P_6, as described in proof of Theorem 7.

Following the same analysis as in previous theorems, we obtain $R_9 > \tau^{-2}$. Hence, deflating χ_m and rescaling the deflated tiles by τ^2 produces a tiling with $\rho_C' = \tau^2 R_{DC} \rho_C$ which is strictly greater than ρ_C. How much so? Suppose we parametrize the fractional excess of ρ_C over ρ_C^0 as

$$\rho_C = \rho_C^0 (1+\alpha). \tag{1}$$

Then, since

$$\rho_C (\tau^4 - R_g \tau^2) \leqslant 1,$$

we have

$$R_g \geqslant \left(\frac{1+\tau^4 \alpha}{1+\alpha} \right) \Big/ \tau^2; \tag{2}$$

consequently, the increase in C clusters under deflation is $\rho_C' = \tau^2 R_{DC} \rho_C = \rho_C^0 (1+\tau^4 \alpha)$. Repeated deflations would lead to an unbounded density [$\rho_C^0 (1+\tau^{4n}\alpha) > \rho_C$ as $n \to \infty$], which is impossible.

Now let us show that the Penrose tiling is the unique tiling with $\rho_C = 1/(3\tau+1)$. If a tiling has C-cluster density $\rho_C = \rho_C^0$ (the Penrose value), then $R_{DC} = \tau^{-2}$ and the C-cluster density in the deflated tiling must equal the Penrose value from the same arguments given in Theorem 1, . . . ,8, Suppose there were a non-Penrose tiling with the same density. We have shown that the only local configurations which can increase the density above the Penrose value are DC clusters, and that the increase in density is due to the B overlap of C-kites, which is the same per DC cluster. Now, the hypothetical tiling has the same density of DC clusters and, hence, the same density of B overlaps surrounded by DC clusters as Penrose tiling. However, by definition, the non-Penrose tiling must also have patches with nonzero area measure which violate the Penrose matching rules, and so cannot belong to the C-kite of any C cluster. Since the DC-cluster density is the same but there are these patches, the average area per C cluster must be less than the Penrose density. A conceivable exception is if there happen to be additional B overlaps which do not belong to DC clusters whose overlap area exactly compensates the area of the patches. Even this possibility can be eliminated because the corollary states that $R_{DC} = 1/\tau^2$, which means that the density of C clusters remains unchanged under deflation and rescaling. Yet, the patches grow: a patch excluded from a C cluster must also be excluded from a DC cluster, but, also, some C clusters that border the patches cannot be part of a DC cluster and add to the patch area. Since the number of C clusters remains fixed but the patches grow, the C-cluster density in the deflated tiling must be less than the Penrose value. This contradicts the corollary; hence, uniqueness is established.

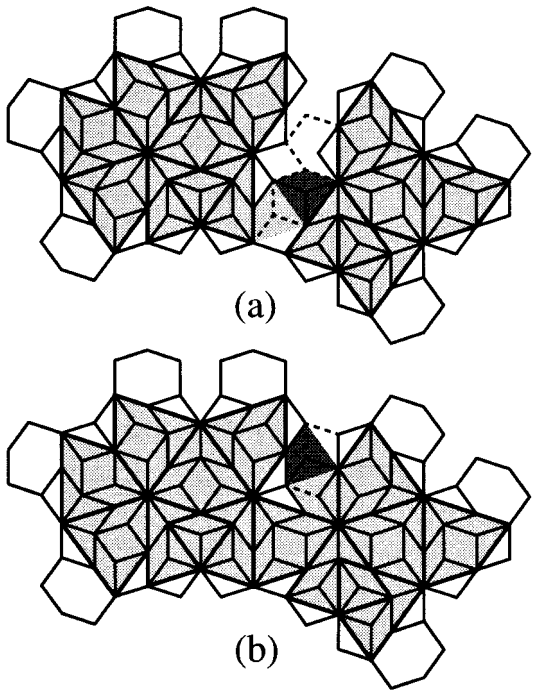

FIG. 15. Assignment of P_7 in (a) and P_8 in (b) for special cases described in proofs of Theorems 8 and 1.

C. Is the *C* cluster unique?

The particular choice of C cluster considered in this paper is not the unique cluster whose density is maximal in a Penrose tiling. (It was chosen primarily because it makes for the simplest proof.) As a simple example, consider the cluster C' which consists of C plus an additional side hexagon, as shown in the right most cluster of Fig. 3(d). In a perfect Penrose tiling, every C cluster lies within a C' cluster. Due to the one-to-one correspondence between the two types of clusters, the density of C clusters and C' clusters are the same in Penrose tiling. On the other hand, the density of C' clusters cannot be greater than that of C cluster in any non-Penrose tiling because every C' cluster guarantees a C cluster. The consequence of this observation is that Penrose tiling has the maximum density of C' clusters as well as C cluster. Or, equivalently, maximizing the density of C' clusters also forces a Penrose tiling.

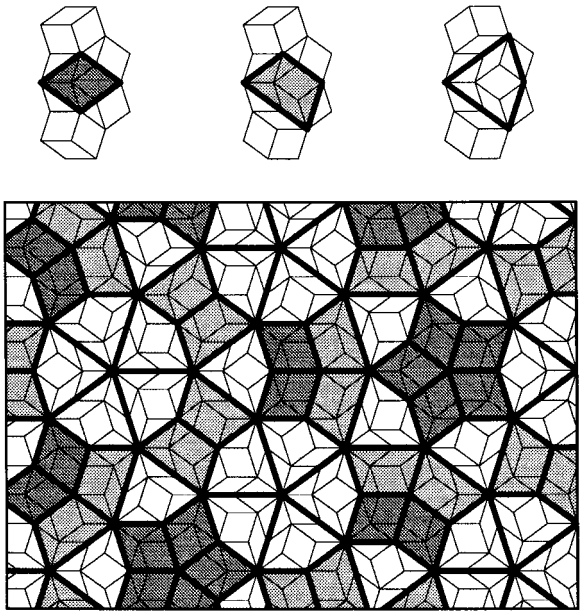

FIG. 16. A core area assignment that differs from the C-kites considered in the proof. Each C cluster in a tiling can be assigned a rhombus-, trapezoid-, or kite-shaped core area depending on whether it is of type $C_{(a,b,c)}$. In a perfect Penrose tiling, these join to form a plane-filling tiling without holes or overlaps, as shown in the figure. This assignment of core area differs from the construction used in the proof which assigns the same C-kite core area to each C cluster. Different assignments are used to explore how different ways of assigning energy per cluster can lead to the same final structure.

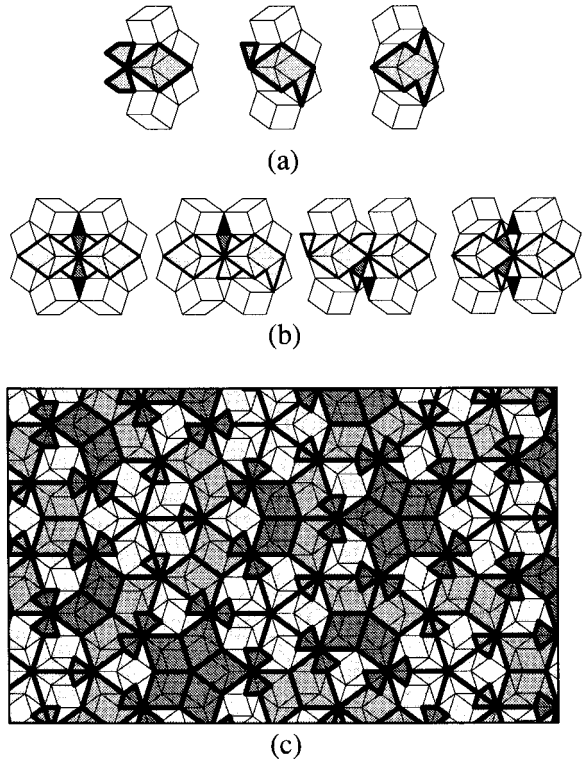

FIG. 17. A third core area assignment for C clusters leading to a different prescription for assigning energy per cluster. The core area depends on whether a given C cluster is of type $C_{(a,b,c)}$. For certain arrangements, shown in (b), the core areas can overlap. For these configurations, though, it is possible to assign the overlap area to one of the C-cluster pair and a different region of the same area (black) to the other cluster. With this rule, the assigned core area are $a_a=2\tau+3$ for C_a, $a_b=5/2\tau+3/2$ for C_b and $a_c=3\tau+1$ for C_c for any C cluster in a Penrose or non-Penrose arrangement. In a perfect Penrose tiling, the special cases shown in (b) do not occur; that is, the core areas as assigned in (a) join to form a plane-filling tiling without holes or overlaps as shown in (c).

D. Maximum density and energetics

We have proven that maximizing the density of C clusters forces a perfect Penrose tiling. The notion is that the cluster represents a low-energy atomic cluster and that minimizing the energy naturally maximizes the density. What kind of Hamiltonian is needed so that the minimum energy configuration is the one that maximizes the C-cluster density?

A simple Hamiltonian with this property is one that assigns energy $-\epsilon(\epsilon>0)$ to every C cluster and zero energy to all other clusters. It is obvious that the ground state of this Hamiltonian has the maximum density of C clusters. However, this choice is not unique.

As an example, we illustrate a Hamiltonian which assigns C clusters different energies depending on the orientations of their side hexagons (which is the same as assigning different energies according to their local environments). In Fig. 16, we show each of the three types of C clusters and introduce a way of assigning core areas, using a different shape for C_a through C_c. This differs from the assignment in the previous sections which assigns the same C-kite core area to each C cluster. Now, consider a Hamiltonian which assigns $\epsilon_a=-\gamma\tau^3$ to a C_a, $\epsilon_b=-\gamma(\tau^3+\tau^4)/2$ to a C_b and $\epsilon_c=-\gamma\tau^4$ to a C_c cluster and zero for all other clusters. These choices of ϵ_i are proportional to the magnitudes of the respective core areas per C cluster for each given type, a_i. If N_i, $i=a$, b, or c is the number of C clusters of type i, the total energy of a configuration is $-\Sigma N_i\epsilon_i\propto-\Sigma N_i a_i$, which is the total area occupied by the union of all core areas. The energy density is minimized by the configuration whose core areas have the greatest fractional coverage of the plane. The Penrose tiling is the unique tiling in which the core areas cover 100% of the total plane. Consequently, the Penrose tiling must be the ground state of the Hamiltonian.

A second, similar example is shown in Fig. 17. In this case, the core area assignment is a little more complicated. First, as can be seen from (a), parts of the ''core area'' lie outside the C cluster itself. This technical difference does not affect our argument, though. Second, there are certain configurations, shown in (b), for which the core areas overlap, unlike the case of Fig. 16. In these cases, though, an alternative assignment is possible, as shown in (b), such that the assigned core area are $a_a=2\tau+3$ for C_a, $a_b=5/2\tau+3/2$ for C_b and $a_c=3\tau+1$ for C_c for any C cluster. For the particular case of a perfect Penrose tiling, the core areas as assigned in (a) never overlap [so the subsidiary rule in (b) does not have to be invoked]; instead, the core areas join to form a plane filling tiling without holes. Consequently, technical differences aside, the situation is the same as in Fig. 16 except that the area assignments are different for $C_{(a,b,c)}$. This enables us to choose a different energy assignment, $\epsilon_a=-\delta(2\tau+3)$, $\epsilon_b=-\delta\{(5\tau+3)/2\}$, and $\epsilon_c=-\delta(3\tau+1)$, such that the Penrose is, again, the unique ground state of the Hamiltonian.

Since the Penrose tiling is the ground state of three different Hamiltonians (one which assigns $-\epsilon$ to all C clusters and two linearly independent choices which assign different energies to C clusters in different local environments), the Penrose tiling is also the ground state of any linear combination of the three Hamiltonians (provided ϵ, γ and δ are positive. So, in the three-dimensional parameter space (ϵ_a, ϵ_b, ϵ_c), there is a three-dimensional region of nonzero measure for which the Hamiltonian maximizes C-cluster density and selects the Penrose tiling for the ground state.

We note that the proofs that the two other Hamiltonians have a Penrose-tiling ground state stand independently of our central proof that Penrose tiling has the maximum density of C clusters. We have approached our investigation from the point-of-view that maximizing the density is a simple and natural criterion, and so we have made this result our focus. However, others may consider the corresponding energetics assignment in which all C clusters have the same energy to be artificial since different C clusters have different local environments. Here, we have shown that the two points-of-view are not contradictory—the Penrose tiling emerges either way.

We speculate that the Penrose ground state is stable under even a wider class of Hamiltonians in which nonzero energy is assigned to other types of tile clusters provided their assigned energy, κ_i satisfies $|\kappa_i| \ll \epsilon$. Suppose one tried to introduce a small, nonzero κ_X to increase the density of a certain cluster X (not C) with respect to its density in a perfect Penrose tiling. The density would be increased only by creating Penrose mismatches, which destroy one or more C clusters each. That is, for every few X's gained, one or more C clusters would be destroyed. An energy proportional to κ_i would be gained for each added X, but this would be accompanied by a loss of energy proportional to ϵ for each C cluster that is destroyed. It seems that there must be a finite band of $|\kappa|_i \ll \epsilon$ for which the Penrose tiling is preserved as the ground-state configuration.

The last speculation, along with the rigorous results above, strongly suggest that there is a robust range of Hamiltonians which maximize C-cluster density and pick out the Penrose tiling as the ground state. The principal requirement for the Hamiltonian is that C clusters have low energy, a condition similar to the condition that determines crystal structure. It seems that the ground state does not depend sensitively on other details, such as whether other clusters have the same or different energies or whether all C clusters have the same energy or different energies. This is a significant improvement over the old Penrose tiling picture based on two types of tiles and matching rules, which seemed to require delicate tuning of Hamiltonian parameters.

We note that the models we have been considering in this section begin with two rhombus tiles (without matching rules) as fundamental building blocks. We were seeking the ground state among all possible configurations of these tiles. This approach is convenient for comparing with the Penrose matching rule model and the random tiling model, both of which are constructed from rhombus tiles. An open issue is whether the presumption of two building blocks, rhombus or otherwise, is necessary.

IV. CONCLUDING REMARKS

Although the results of this paper are mathematical in nature, they have several important implications for the physics of quasicrystals. First, the decagon construction shows that the atomic structure of a quasicrystal can be characterized in terms of the decoration of a single cluster, rather than two clusters as the Penrose tiles would suggest. Furthermore, the single cluster has to have the property that it can share atoms with neighbors in accordance with overlaps. This greatly simplifies the problem of searching for structural models for quasicrystals. It immediately applies to three-dimensional decagonal quasicrystals, where decagonal prisms would replace the decagons. The analog of the decagon for icosahedral quasicrystals is the triacontrahedron.

Second, the constructions imply a closer tie between quasicrystals and crystals. Now one can say that both can be described in terms of the packing of a single cluster. In a crystal, the cluster is called the unit cell, and it packs edge-to-edge with its neighbors. In this picture, quasicrystals correspond to a generalization in which the ''unit cells'' overlap. In both cases, the formation of the particular structure may be described in terms of a low-energy atomic cluster. Hence, perhaps one heads towards a more unified picture of ordered solids.

Third, the constructions imply a simpler explanation of why quasicrystals form, shedding, new light on an old mystery. They make it plausible that quasicrystals can be understood by considering the energetics of microscopic clusters and that cluster overlap is an important structural element. The atomic structures of known quasicrystals include atom clusters which can share atoms using geometries analogous to those considered here.[5] This has motivated several closely related models of quasicrystals based on clusters.[8,12–15]

Our concept can be tested by studying theoretically the energetics of atom clusters found in real quasicrystals. One can use total-energy calculations to estimate the energetics of the clusters and to test if overlap is energetically preferred. Perhaps the modeling studies will lead to suggestions for new quasicrystals. The second construction scheme, in addition to posing an explanation of why quasicrystals form, also suggests a kinematic mechanism to explain how they form: namely, by local atomic rearrangement that increases the local density of some certain atom cluster which then forces quasicrystallinity. From future structural and kinematical studies of known quasicrystals, these principles may be established, perhaps enabling the reliable prediction of new quasicrystals.

ACKNOWLEDGMENTS

We thank F. Gähler for bringing P. Gummelt's work to our attention and for many helpful comments and criticism. We also thank P. Gummelt for sharing her results prior to publication and for suggestions regarding this paper. J. Socolar has also provided important suggestions. This research was supported by the Department of Energy Grant No. DOE-EY-76-C-02-3071 at Penn (P.J.S.) and by the National Science Foundation Grant No. NSF-DMR-96-32521 at Maryland (H.C.J.).

[1] D. Levine and P. J. Steinhardt, Phys. Rev. Lett. **53**, 2477 (1984).
[2] R. Penrose, Bull. Inst. Math. Appl. **10**, 266 (1974).
[3] A. Kortan, R. Becker, F. Thiel, and H. Chen, Phys. Rev. Lett. **64**, 200 (1989).
[4] R. Becker and A. Kortan, in *Quasicrystals, The State of Art*, edited by D. P. DiVincenzo and P. J. Steinhardt (World Scientific, Singapore, 1991), pp. 111–132.
[5] C. L. Henley, in *Quasicrystals, The State of Art* (Ref. 4), pp. 429–524.
[6] P. Gummelt, Geometriae Dedicata **62**, 1 (1996).
[7] P. J. Steinhardt and H.-C. Jeong, Nature (London) **382**, 433 (1996).
[8] H.-C. Jeong and P. J. Steinhardt, Phys. Rev. Lett. **73**, 1943 (1994).
[9] P. Steinhardt, Am. Sci. **74**, 586 (1986).
[10] N. G. de Bruijn, Nederl. Akad. Wetensch. Proc. A **84**, 1 (1981).
[11] M. Gardner, Sci. Am. **236**, 110 (1977).
[12] J. L. Aragon, D. Romeu, and A. Gomez, Phys. Rev. Lett. **67**, 614 (1991).
[13] S. Burkov, J. Phys. (Paris) **2**, 695 (1992); Phys. Rev. Lett. **67**, 614 (1991).
[14] W. Steurer, T. Haibach, B. Zhang, S. Kek, and R. Luck, Acta Crystallogr. B **49**, 661 (1993).
[15] C. Janot and M. de Boissieu, Phys. Rev. Lett. **72**, 1674 (1994).